

The magnetic structure in the antiferromagnetic phase of $\text{Ce}(\text{Fe}_{1-x}\text{Co}_x)_2$

This article has been downloaded from IOPscience. Please scroll down to see the full text article.

1989 J. Phys.: Condens. Matter 1 629

(<http://iopscience.iop.org/0953-8984/1/3/014>)

View [the table of contents for this issue](#), or go to the [journal homepage](#) for more

Download details:

IP Address: 171.66.16.90

The article was downloaded on 10/05/2010 at 17:01

Please note that [terms and conditions apply](#).

The magnetic structure in the antiferromagnetic phase of $\text{Ce}(\text{Fe}_{1-x}\text{Co}_x)_2$

S J Kennedy[†], A P Murani[‡], J K Cockcroft[‡], S B Roy[†] and B R Coles[†]

[†] Blackett Laboratory, Imperial College, London SW7 2BZ, UK

[‡] Institut Laue–Langevin, 156X, 38042 Grenoble Cédex, France

Received 15 July 1988

Abstract. The nature of the low-temperature ($T \approx 90$ K) magnetic phase transition in cubic Laves-phase $\text{Ce}(\text{Fe}_{1-x}\text{Co}_x)_2$ compounds with $x = 0.15, 0.20$ has been determined using powder neutron diffraction measurements. Below this temperature, ferromagnetism is replaced by an antiferromagnetic phase, which consists of (111)-type sheets with parallel spins and antiparallel coupling of spins between adjacent (111) sheets. The orientation of the magnetic moments could not be uniquely determined; however, they are oriented within a cone that is defined by $\sin^2 \varphi = \frac{2}{3}$ relative to the (111) sheets and includes the (Fe, Co) sublattice nearest-neighbour directions. No difference in magnitude between the (Fe, Co) sublattice moments of the two phases could be detected, nor was any significant magnetic moment detected at the Ce sites in either phase. High-resolution neutron diffraction measurements show that the application of large magnetic fields (≈ 4 T) in the antiferromagnetic phase restores ferromagnetism and removes the associated structural distortion.

1. Introduction

The nature of the anomalous magnetic properties of CeFe_2 (low T_c and magnetisation) relative to the ferrimagnetic RFe_2 ($\text{R} = \text{Sm, Gd, Tb, Dy, Ho, Er, Tm}$) and the ferromagnetic MFe_2 ($\text{M} = \text{Sc, Zr, Y, Hf, Lu}$) Laves-phase compounds has been the subject of considerable interest for many years (Buschow and van Stapele 1971, Buschow 1977, Hilscher 1982). This interest has recently been renewed by reports of the breakdown of ferromagnetism at low temperatures in the pseudo-binary $\text{Ce}(\text{Fe}_{1-x}\text{M}_x)_2$ compounds, where ($\text{M} = \text{Co, Al, Ru}$). In these compounds, as Fe is progressively substituted for by Co, Al or Ru, the low-temperature magnetic behaviour suggests that ferromagnetism gives way to a canted spin structure, via partial loss of ferromagnetism initially; and that as more Fe is replaced this canted spin structure reaches a point where total loss of ferromagnetism is observed.

Observations of the breakdown of ferromagnetism in specific $\text{Ce}(\text{Fe}_{1-x}\text{M}_x)_2$ compounds have been reported for $\text{M} = \text{Co}$ by Rastogi and Murani (1987), for $\text{M} = \text{Al}$ by Franceschini and da Cunha (1985) and Roy and Coles (1987), and for $\text{M} = \text{Ru}$ by Roy and Coles (1988). In the wake of these reports, high-resolution neutron powder diffraction measurements on $\text{Ce}(\text{Fe}_{0.8}\text{Co}_{0.2})_2$ and $\text{Ce}(\text{Fe}_{0.96}\text{Ru}_{0.04})_2$ (Kennedy *et al* 1988a, b) have shown that this low-temperature magnetic transition is accompanied by

a small structural distortion to rhombohedral symmetry ($\alpha \approx 90.20^\circ$) with a decrease of about 0.05% in cell volume.

We report the results of a detailed neutron diffraction study aimed at determination of the nature of the magnetic ordering in the low-temperature phase. The compounds studied, $\text{Ce}(\text{Fe}_{1-x}\text{Co}_x)_2$ with $x = 0.15, 0.20$, are those in which ferromagnetism disappears completely at low temperature ($T \approx 90$ K).

2. Experiment

The preparation of the two $\text{Ce}(\text{Fe}_{1-x}\text{Co}_x)_2$ compounds ($x = 0.15, 0.20$) was carried out as we have described previously (Kennedy *et al* 1988b). Diffraction measurements in the temperature range 5 to 280 K were performed on the neutron powder diffractometer D1B at the ILL, where the 400-cell multidetector spans 80° , with five cells per degree. The measuring time was approximately nine minutes per diffraction pattern. The incident wavelength of 2.52 Å allowed observation of the first four nuclear reflections and the first six antiferromagnetic reflections. Further diffraction measurements were performed on the D2B high-resolution powder diffractometer (at ILL), where the greater angular resolution allowed observation of the associated structural distortion. This spectrometer has 64 detectors spanning 160° in 2θ . Measurements were taken at intervals of 0.025° in 2θ at a wavelength of 1.595 Å with a measuring time of approximately 40 minutes per diffraction pattern. The response of the system to external magnetic fields of up to 4 T was determined using a cryomagnet.

3. Results and analysis

A plot showing the temperature dependence of the diffraction pattern obtained on D1B for $\text{Ce}(\text{Fe}_{0.8}\text{Co}_{0.2})_2$ is shown in figure 1. The temperature ranges from 65 to 105 K in steps of approximately 0.5° . The four intense peaks are the nuclear $(111)_n$, $(220)_n$, $(311)_n$ and $(222)_n$ reflections of the C_{15} lattice as marked. The loss of ferromagnetism at about 85 K is clearly indicated by the drop in intensity of these reflections (excepting $(220)_n$) as the ferromagnetic contribution disappears. This temperature range marks the appearance of a set of small antiferromagnetic reflections—indexed in the figure as $(111)_m$, $(3\bar{1}\bar{1})_m$, $(3\bar{3}\bar{1})_m$, $(333, 511)_m$ and $(5\bar{3}\bar{1})_m$. The apparent discrepancy between ferromagnetic and antiferromagnetic intensities is explained by the low multiplicity and magnetic structure factor of the antiferromagnetic reflections combined with a slight peak broadening due to the rhombohedral distortion that accompanies this magnetic transition. The contribution of the structural distortion to the drop in intensity can be gauged by the effect seen at $(220)_n$ —this peak is due solely to Bragg scattering from the Ce sublattice and has a negligible magnetic contribution. The extra reflections (labelled ‘imp’) some of which coincide with the antiferromagnetic reflections, are consistent with nuclear reflections from 1–2% iron-rich impurity, with space group $R3m$ ($\text{Ce}_2\text{Fe}_{17}$).

In order to interpret the observed antiferromagnetic reflections, we view the C_{15} lattice as six interpenetrating FCC lattices, with four basis points for (Fe, Co) sites and two basis points for Ce sites. The antiferromagnetic reflections are then consistent with antiferromagnetic ordering in which the magnetic lattice constant (a_m) is twice the atomic lattice constant and the magnetic moments of an FCC basis are parallel within the (111)

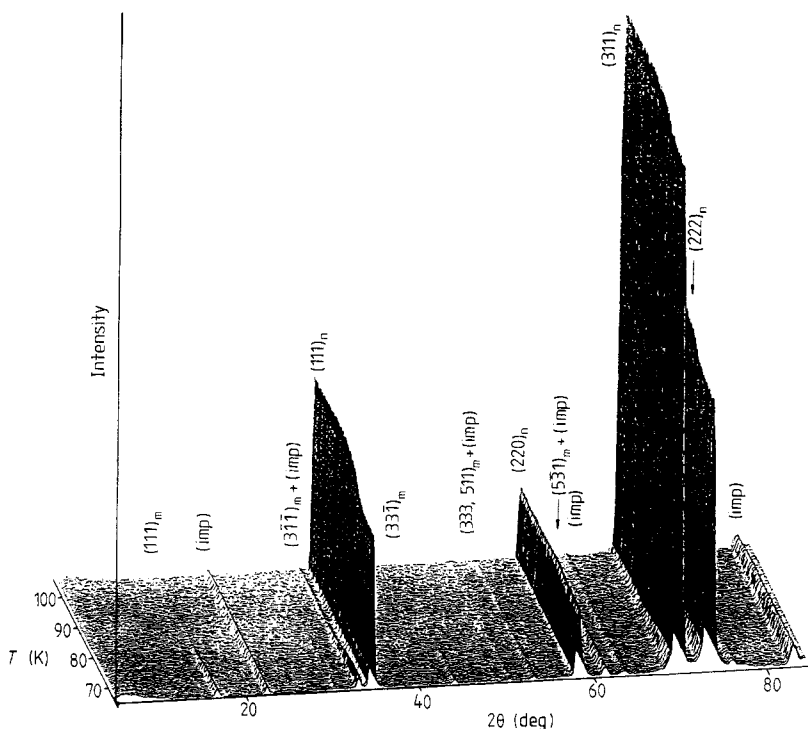


Figure 1. The D1B neutron powder diffraction pattern from $Ce(Fe_{0.8}Co_{0.2})_2$ between 65 and 105 K, showing ferromagnetic–antiferromagnetic phase transition at about 85 K. Nuclear peaks are labelled with subscript n ; antiferromagnetic peaks are labelled with subscript m . Extra reflections (labelled (imp)) are consistent with 1–2% Ce_2Fe_{17} impurity.

planes but antiparallel between adjacent (111) planes. This type of antiferromagnetic order is seen in the 3d transition-metal oxides—MnO, FeO, CoO, NiO (Roth 1958).

The magnetic structure factor for such an arrangement of spins, with average magnetic moment $\bar{\mu}$, within a face-centred cubic lattice of volume $(2a_0)^3$ is

$$F'_m(hkl) = \begin{cases} 32\bar{\mu} & hkl \text{ all odd, such that } h+k, h+l, k+l = 4n+2 \\ 0 & \text{otherwise.} \end{cases}$$

Thus reflections are predicted for all combinations where hkl are all odd, but with multiplicity reduced by a quarter relative to the multiplicity of the ferromagnetic reflections of the high-temperature phase. The total magnetic structure factor for the Laves phase also includes the interference ($F''_m(hkl)$) between scattering from the six FCC basis points:

$$F_m(hkl) = F'_m(hkl)F''_m(hkl).$$

We may simplify the interference term by disregarding contributions from the Ce sublattice. This simplification is justified on the basis that no magnetic scattering from the Ce sites is detected in the ferromagnetic phase. The relative positions of the (Fe, Co) sublattice basis points are $\langle 000 \rangle$, $\langle 110 \rangle a_m/8$, $\langle 101 \rangle a_m/8$ and $\langle 011 \rangle a_m/8$; and the centre of

Table 1. Average sublattice magnetic moments, moment orientations and transition temperatures for $\text{Ce}(\text{Fe}_{1-x}\text{Co}_x)_2$.

Cobalt fraction (x)	Ferromagnetic moment ≈ 100 K ($\mu_B/3d$ atom)	Antiferromagnetic moment ≈ 20 K ($\mu_B/3d$ atom)	φ angle to (111) plane	T_N (K)
0.15	1.1 ± 0.1	1.1 ± 0.1	$53^\circ \pm 4^\circ$	94 ± 1
0.20	1.0 ± 0.1	1.0 ± 0.1	$53^\circ \pm 5^\circ$	90 ± 1

magnetic symmetry is at $\langle 111 \rangle a_m/8$, so $F_m''(hkl) = \sqrt{2}$, for reflections that satisfy the above Bragg conditions, and $F_m(hkl) = 32\sqrt{2}\bar{\mu}_{\text{Fe}}$ /per unit cell of volume a_m^3 .

The orientation of the antiferromagnetic moments relative to the scattering plane is included in the magnetic intensity (I_m), since $I_m \propto q^2 F_m^2(hkl)$ and $q^2 = 1 - (\hat{\mu} \cdot \hat{k})^2 = \sin^2 \alpha$, where $\hat{\mu}$ and \hat{k} are unit vectors describing the magnetic moment and scattering vectors respectively. If we define φ as the angle between μ and the (111) plane we find that

$$\overline{q^2(111)} = \cos^2 \varphi$$

$$q^2(3\bar{1}\bar{1}) = \alpha + \beta \sin^2 \varphi \quad (\alpha = \frac{17}{33}, \beta = \frac{5}{11}).$$

Thus the ratio $\overline{q^2(111)}/\overline{q^2(3\bar{1}\bar{1})}/\overline{q^2(3\bar{1}\bar{1})}$ can be used to determine φ , which is the angle of the cone defining the magnetic moment orientation relative to the (111) plane.

The D1B diffraction patterns have been summed over about 25 diffraction patterns in order to obtain representative patterns, with improved statistical quality, for the ferromagnetic and antiferromagnetic phases. These summed diffraction patterns were least-squares fitted to Gaussian lineshapes to extract the integrated intensities—from which the ferromagnetic and antiferromagnetic moments were calculated. The ferromagnetic moments were calculated from the difference between the integrated intensities of the $(111)_n$ and $(220)_n$ peaks in the ferromagnetic and antiferromagnetic phases. In the case of the $(220)_n$ peaks the intensity difference corresponds to a Ce moment of $<0.1 \mu_B/\text{atom}$, assuming a Ce^{3+} form factor (Stassis *et al* 1977); so the ferromagnetic moments of the (Fe, Co) atoms were calculated assuming zero Ce moment and are presented in table 1.

In order to calculate the antiferromagnetic sublattice magnetic moments, the angle φ was first determined using the method described above. The resultant angles are included in table 1 along with the antiferromagnetic moments, which are calculated from the integrated intensities of both the $(111)_m$ and $(311)_m$ peaks of the antiferromagnetic phase.

The table clearly shows that the (Fe, Co) sublattice magnetic moments are stable in magnitude through the transition, in agreement with the findings of Pillay *et al* (1988). We have established that there is no detectable magnetic moment at the Ce sites in the ferromagnetic phase. If there were an ordered magnetic moment at the Ce sites in the antiferromagnetic phase, we would expect to see this as an added contribution to the average antiferromagnetic sublattice moment. That this contribution is not seen indicates that Ce-site magnetic ordering is not responsible for this transition.

The average angle of the moments to the (111) plane includes the high-symmetry (Fe, Co) nearest-neighbour direction, at the $\langle 110 \rangle$ -type positions. To preserve rhombohedral

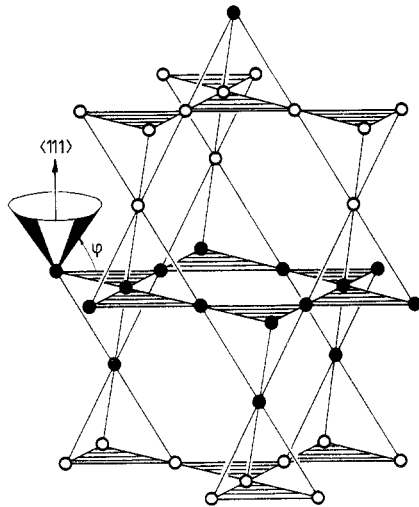


Figure 2. The distribution of (Fe, Co) sublattice atoms in the cubic Laves-phase $Ce(Fe, Co)_2$, showing stacking of tetrahedra in $\langle 111 \rangle$ -type planes. Full circles denote spins up and open circles denote spins down relative to the $\langle 111 \rangle$ plane. The spins lie in a cone defined by $\sin^2 \varphi = \frac{2}{3}$, which includes the 'out-of-plane' $\langle 110 \rangle$ -type nearest-neighbour directions (as indicated).

symmetry, we require that all three directions— $\langle 110 \rangle$, $\langle 101 \rangle$ and $\langle 011 \rangle$ —are equally populated. Indeed if this is the case, we may describe the spin arrangement of the antiferromagnetic phase as indicated in figure 2—where the (Fe, Co) sites are shown stacked in the $\langle 111 \rangle$ planes.

In the series of powder diffraction measurements, using the high-resolution neutron diffractometer (D2B), we were able to verify the structural distortion seen on HRPD (at the Rutherford Appleton Laboratories), as well as observing the antiferromagnetic phase described above. These measurements showed that the temperatures of the structural and magnetic transitions coincide to within 1° —these transition temperatures are included in table 1. The diffraction patterns were subjected to Rietveld refinements with atomic coordinates for Ce at the $8a$ site $(0, 0, 0)$ and for Fe, Co at the $16d$ site $(\frac{3}{8}, \frac{5}{8}, \frac{3}{8})$ using the cubic space group ($Fd\bar{3}m$) in the ferromagnetic phase and the rhombohedral space group ($R\bar{3}m$) in the antiferromagnetic phase. Figure 3 shows the fit of the rhombohedral lattice to the antiferromagnetic phase at $T = 5$ K (figure 3(a)), and the fit of the cubic lattice to the ferromagnetic phase at $T = 98$ K (figure 3(b)), for the $Ce(Fe_{0.85}Co_{0.15})_2$ powder. The antiferromagnetic diffraction pattern can be extracted from the difference spectra (lower curves). The Rietveld refinements indicated a rhombohedral distortion, which reaches $\alpha = 90.26^\circ \pm 0.01^\circ$ at 5 K for both powders. The temperature dependence of the rhombohedral distortion was consistent with that seen on HRPD.

We also observed, on D2B, the structural and magnetic response of both powders to an external magnetic field. A magnetic field of 4 T applied at temperatures of 70 K and above was sufficient to both restore ferromagnetic order and remove the structural distortion in the $x = 0.20$ powder. At temperatures of 60 K and below no field dependence was observed. Similar results were obtained for the $x = 0.15$ powder. That an

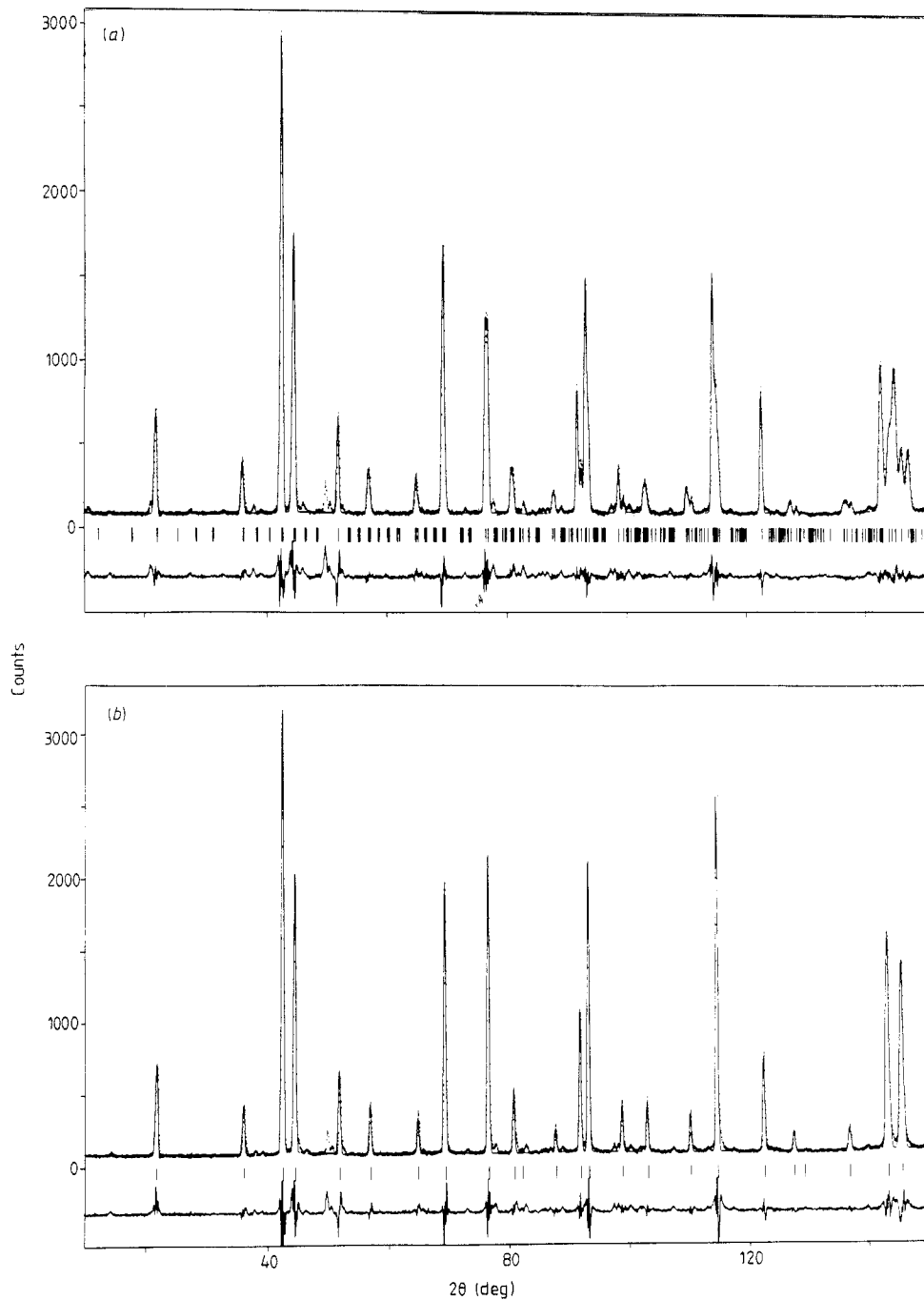


Figure 3. The Rietveld refinements of neutron diffraction patterns for $x = 0.15$ powder on D2B. The full curve shows the fit of (a) the rhombohedral structure at $T = 5$ K, with $a_0 = 7.2717 \pm 0.0001$ Å and $\alpha = 90.26^\circ \pm 0.01^\circ$; and (b) the cubic structure at $T = 98$ K, with $a_0 = 7.2749 \pm 0.0002$ Å. Lower curves show the difference between the results from experiment and fitting—extra reflections common to both patterns are consistent with 1–2% $\text{Ce}_2\text{Fe}_{17}$ impurity. The reflections seen only in (a) are antiferromagnetic.

external magnetic field can reverse both transitions shows that the magnetic properties are active in this transition.

4. Discussion

These measurements have clearly established that ferromagnetic ordering in this system is replaced at low temperatures by long-range antiferromagnetic order rather than a quasi-random spin freezing as suggested by Pillay *et al* (1988), and they have also supplied much detail as to the type of antiferromagnetic order present. The orientation of the magnetic moments to the unique (111) planes ($\sin^2 \varphi = \frac{2}{3}$) may correspond to the high-symmetry $\langle 110 \rangle$ -type (Fe, Co) nearest-neighbour direction. On the other hand, it may be more than coincidental that this angle can be correlated with the nuclear spin angle measured by Atzmony and Dariel (1974) in the range $150 < T < 210$ K for ferromagnetic $CeFe_2$. In their Mössbauer transmission measurements, they deduce a spin reorientation at 150 K from the $\langle 100 \rangle$ axes to a cone of about 20° to the $\langle 100 \rangle$ axes. These two cones combine to give a unique moment direction of $\langle 114 \rangle$ for the Fe atoms, which is also a high-symmetry direction for the cubic Laves phase. More recently a spin reorientation away from the $\langle 100 \rangle$ axes was seen at the ferro-antiferromagnetic transition in Mössbauer transmission studies on $Ce(Fe_{0.85}Co_{0.15})_2$ and $Ce(Fe_{0.75}Co_{0.25})_2$ powders by Pillay *et al* (1988).

The $\langle 111 \rangle$ symmetry of the antiferromagnetic phase is reminiscent of the commensurate component of the antiferromagnetic ordering of the Ce atoms in isostructural $CeAl_2$, with a localised moment of about $0.63 \mu_B/Ce$ atom and no Al moment (Barbara *et al* 1979, Shapiro *et al* 1979). However, in $CeAl_2$ the lattice constant of 8.06 \AA is characteristic of Ce^{3+} with local 4f moments, whereas in $CeFe_2$ the lattice constant of 7.30 \AA is characteristic of an itinerant 4f contribution (Eriksson *et al* 1988).

In our earlier report of neutron diffraction measurements on $Ce(Fe_{0.8}Co_{0.2})_2$ (Kennedy *et al* 1988a, b) we suggested that the spin reorientation from $\langle 100 \rangle$ to $\langle 111 \rangle$ symmetry would provide a mechanism for the observed rhombohedral distortion via the magneto-elastic coupling model of Cullen and Clark (1977). A prerequisite for this model is a 4f magnetic moment on the Ce sites. The role of the f-electron character is supported by the observation of a rhombohedral distortion at the Curie temperature in UFe_2 (Popov *et al* 1980). A recent itinerant electron theory (self-consistent linear muffin-tin orbital calculations) for $CeFe_2$ (Eriksson *et al* 1988) yields a magnetic moment of $-0.7 \mu_B$ (antiparallel to Fe), composed of $-0.4 \mu_B$ 4f and $-0.3 \mu_B$ 5d contributions. Also self-consistent energy band calculations for $ZrFe_2$ and YFe_2 (Mohn and Schwartz 1985) as well as experiments (pressure dependence of magnetisation) by Armitage *et al* (1986) suggest that both Zr and Y possess a small magnetic moment of about $-0.5 \mu_B$. This contrasts with the negligible moment on Lu in $LuFe_2$ obtained from magnetisation density measurements on a single crystal by Givord *et al* (1980).

As mentioned above, the present study returns a negligible magnetic moment ($< 0.1 \mu_B$) at the Ce sites in both the ferromagnetic and antiferromagnetic phases, so the observed spin reorientation and rhombohedral distortion must have another driving force. This result also highlights the difference from the theoretical calculations of the Ce moment in $CeFe_2$ and suggests further theoretical and experimental work, e.g. measurement of the form factor (magnetisation density) of Ce when a single crystal of $CeFe_2$ becomes available.

The fact that an applied magnetic field can reverse both the magnetic and structural

transitions shows that the magnetic properties are active in this transition and that the destabilisation of the ferromagnetic order in these alloys, by substitution of Co, Ru or Al, brings about this transition. It may be that a temperature-dependent competition between itinerant exchange interactions and magnetic anisotropy in the 3d sites is responsible for this transition.

Acknowledgments

Our thanks to Dr H E N Stone (IC) for sample preparation. This work is financially supported by the SERC (UK).

References

- Armitage J G M, Dumelow T, Mitchell R H, Reidi P C, Abell J S, Mohn P and Schwartz K 1986 *J. Phys. F: Met. Phys.* **16** L141–4
- Atzmony U and Dariel M P 1974 *Phys. Rev.* **10** 2060–7
- Barbara B, Rossignol M F, Boucherle J X, Schweizer J and Buevoz J L 1979 *J. Appl. Phys.* **50** 2300–7
- Buschow K H 1977 *Rep. Prog. Phys.* **40** 1179–256
- Buschow K H and van Stapele R P 1971 *J. Physique Coll.* **32** C1 672–4
- Cullen J R and Clark A E 1977 *Phys. Rev. B* **15** 4510–5
- Eriksson O, Nordstrom L, Brooks M S S, Johansson B 1988 *Phys. Rev. Lett.* **60** 2523–6
- Franceschini D F and da Cunha S F 1985 *J. Magn. Magn. Mater.* **51** 280–90
- Givord D, Gregory A R and Schweizer J 1980 *J. Magn. Magn. Mater.* **15/18** 293–4
- Hilscher G 1982 *J. Magn. Magn. Mater.* **27** 1–31
- Kennedy S J, Coles B R and Ibberson R M 1988a *Rutherford Appleton Laboratory No* 88–319
- Kennedy S J, Murani A P, Coles B R and Moze O 1988b *J. Phys. F: Met. Phys.* **18** 2499–504
- Mohn P and Schwartz K 1985 *Physica B* **130** 26–8
- Pillay R G, Grover A K, Balasubramanian V, Rastogi A K and Tandon P N 1988 *J. Phys. F: Met. Phys.* **18** L63–8
- Popov Yu F, Levitin R Z, Zeleny M, Deryagin A V and Andreev A V 1980 *Sov. Phys.-JETP* **51** 1223–6
- Rastogi A K and Murani A P 1987 *Proc. 5th Int. Conf. Valence Fluctuations (Bangalore)* (New York: Plenum)
- Roth W L 1958 *Phys. Rev.* **110** 1333–41
- Roy S B and Coles B R 1987 *J. Phys. F: Met. Phys.* **17** L215–20
- 1988 *J. Appl. Phys.* **63** 4094–5
- Stassis C, Deckman H W, Harmon B N, Desclaux J P and Freeman A J 1977 *Phys. Rev. B* **15** 369–76
- Shapiro S M, Gurewitz E, Parks R D and Kupferberg L C 1979 *Phys. Rev. Lett.* **43** 1748–51